KIT

Karlsruhe Institute of Technology

End-to-end simulation of the Extreme Universe Space Observatory (EUSO)

Vollständige Simulation des Extreme Universe Space Observatory (EUSO)

Bachelor Thesis of

Matthias Blaicher

An der Fakultät für Physik
Institut für Experimentelle Kernphysik

Reviewer: Prof. Dr. Johannes Blümer
                Dr. Andreas Haungs
Advisor: Dr. Andreas Haungs

März 2012

Abstract

Ever since the discovery of cosmic rays by Victor Hess [Hes12] in 1912 great efforts have been undertaken to understand the origin of cosmic rays up to the highest energies of 10^{21} eV. A common detection method utilizes the fluorescence light produced in the atmosphere during extensive air showers induced by cosmic rays. Due to the extremely low flux of particles in the ultra high energy domain vast volumes of atmosphere have to be monitored. The largest fluorescence telescope, the Pierre Auger Observatory, is located in Argentina and covers over $3\,000\,\text{km}^2$.

The space based JEM-EUSO mission is a proposed pathfinder mission to further increase the amount of observed atmosphere. The Extreme Universe Space Telescope (EUSO) will be attached to the Japanese Experiment Module (JEM) of the International Space Station (ISS) and provides a high resolution sensor and a wide field of view ($\pm 30°$).

Since early 2003, the Pierre Auger Observatory has been constantly developing the $\overline{\text{Off}}\underline{\text{line}}$ framework. $\overline{\text{Off}}\underline{\text{line}}$ is a comprehensive experimentally verified simulation and reconstruction framework for extensive air showers. Likewise, the EUSO Simulation & Analysis Framework (ESAF) has been developed for the JEM-EUSO mission.

This thesis analyzes the possibility of using the $\overline{\text{Off}}\underline{\text{line}}$ framework in conjunction with the ESAF framework as a possible future standalone simulator for JEM-EUSO.

Within this thesis, it is shown that the $\overline{\text{Off}}\underline{\text{line}}$ framework is able to simulate space based telescopes. Additionally, an $\overline{\text{Off}}\underline{\text{line}}$ to ESAF adapter module has been developed which uses $\overline{\text{Off}}\underline{\text{line}}$ for shower and atmosphere simulation and ESAF for the detector simulation. The module gives comparable results to pure ESAF. An exemplary comparison is given to understand the key differences between the two simulations.

Kurzbeschreibung

Seit der Entdeckung der kosmischen Strahlung durch Victor Hess [Hes12] im Jahre 1912 wurde die Herkunft und Existenz hochenergetischer Strahlung bis zu Energien von 10^{21} eV mit Hilfe unterschiedlichster Experimente untersucht. Eine verbreitete Nachweismethode stellt die Beobachtung des Fluoreszenzlichts ausgedehnter Luftschauer dar. Aufgrund des geringen Teilchenflußes der höchst-energetischen kosmischen Strahlung ist es notwendig, die Atmosphäre großflächig auf Fluoreszenzlicht zu überwachen. Das derzeit größte Fluoreszenzteleskop ist das Pierre Auger Observatory in Argentinien, welches sich über $3\,000\,\mathrm{km}^2$ erstreckt.

Die Menge an überwachter Atmosphäre lässt sich durch Beobachtung aus dem Weltraum stark vergrößern. Die JEM-EUSO Mission ist ein geplantes Weltraumteleskop, welches an dem japanischen Experimentiermodul (JEM) der Internationalen Raumstation (ISS) angebracht werden wird. Das JEM-EUSO Experiment, das als Wegbereiter für eine neue Ära von Detektoren dient, besteht aus einem hochauflösenden Sensor und einem weiten Sichtfeld von $\pm 30°$.

Im Rahmen des Pierre Auger Observatory wird seit Anfang 2003 das $\overline{\text{Off}\underline{\text{line}}}$ Framework entwickelt. Das $\overline{\text{Off}\underline{\text{line}}}$ Framework dient sowohl der Simulation als auch der Rekonstruktion von Ereignissen und wurde ausgiebig mit Messdaten verifiziert. Für das JEM-EUSO Projekt existiert ebenfalls eine Simulation- und Rekonstruktionssoftware, das EUSO Simulation & Analysis Framework (ESAF).

Diese Arbeit untersucht die Möglichkeit, das $\overline{\text{Off}\underline{\text{line}}}$ Framework zur Simulation von JEM-EUSO zu nutzen. Zu diesem Zweck wurde ein Adaptermodul für $\overline{\text{Off}\underline{\text{line}}}$ entwickelt, welches $\overline{\text{Off}\underline{\text{line}}}$ für die Simulation der Atmosphäre nutzt und die propagierten Photonen an ESAF übergibt. Die verbleibende Detektorsimulation wird dann vollständig in ESAF ausgeführt. Dieser neue Simulationszweig gibt vergleichbare Ergebnisse wie eine reine ESAF Simulation, verfügt aber aufgrund der Mächtigkeit des $\overline{\text{Off}\underline{\text{line}}}$-Paketes über wesentlich mehr Variationsmöglichkeiten, sowie über eine konzeptionell modernere und modularere Herangehensweise an eine vollständige Simulation des JEM-EUSO Projektes. Einige Simulationsergebnisse werden in dieser Arbeit exemplarisch verglichen, um die Hauptunterschiede zwischen den beiden Simulationen aufzuzeigen.

Contents

1. Introduction

It has been a hundred years since the discovery of cosmic rays by Victor Hess [Hes12] but the basic questions have remained the same: What is cosmic radiation made of and where does it come from? Particle acceleration by supernova shock fronts is now a well established paradigm, which can partially explain the origin of cosmic rays with energies up to 10^{15} eV. Many theories have been developed to explain the existence of particles with extreme energies up to a few 10^{20} eV, but despite all efforts the basic questions remain.

Cosmic rays produce extensive air showers of billions of secondary particles in the atmosphere, some of which can be detected at ground level. As the shower develops, the secondary particles of extensive air showers produce faint Cherenkov and fluorescence light by interaction with the Earth's atmosphere which can be detected during night-time with photomultipliers. From these measurements it is possible to reconstruct the energy, mass and arrival direction of the primary particle. But research at the highest energies is hampered by the low flux of cosmic rays at these energies thus requiring huge detection areas. Traditionally, this has been solved with vast ground based observatories, such as the Pierre Auger Observatory covering over $3\,000\,\mathrm{km}^2$ in Argentina.

To improve the detection statistics it is mandatory to further increase the amount of monitored atmosphere. One suggestion is to move observation to space and thus increase exposure over several orders of magnitude. The idea of observing extensive air showers from space was already proposed in the late seventies by John Linsley [Lin79]. But only in the last decade there have been deeper studies on this subject. Several iterations of a space based telescope have been proposed. The most recent proposal, JEM-EUSO, is planned to be attached to the Japanese Experimental Module (JEM) aboard the International Space Station in 2015.

The future performance of unbuilt experiments is typically accessed by simulating all relevant physical processes as well as possible. Because of the complexity of ultra-high energy cosmic rays physics and their observation principle large and complex simulation programs are needed. In the past, each experiment has written its own simulation software with its own strengths and weaknesses. This thesis facilitates the proven $\overline{\text{Off}}\underline{\text{line}}$ simulation framework developed at the Pierre Auger Observatory and investigates the possibility to use it for space based observations. In this thesis it is shown that $\overline{\text{Off}}\underline{\text{line}}$ is indeed able to simulate a satellite configuration which is used in JEM-EUSO. The $\overline{\text{Off}}\underline{\text{line}}$ simulation framework might ultimately provide the basis of a unified air shower simulation framework which is thoroughly tested and avoids duplicate coding effort.

2. Ultra-High Energy Cosmic Rays and observation methods

2.1. Cosmic rays

Cosmic ray science is a very wide topic which is deeply rooted in many fields of physics, ranging from nuclear and particle physics to astrophysics and cosmology. Moreover, modern elementary particle physics in accelerators has evolved from studies of elementary particle processes in cosmic radiation. Before the second half of the 20th century it presented the only way of experimenting with high energy radiation and even today the strongest accelerators are outmatched by the energy of ultra-high energy cosmic rays.

The era of cosmic rays began in the first decade of the twentieth century when Victor Hess set out to investigate the mystery of rising levels of ionizing radiation with increasing altitude. After he published his findings in 1912 [Hes12] the sparked interest led to further discoveries by Walther Bothe, Werner Kolhörster and later Pierre Auger [AEM+39]. By investigating absorption characteristics they concluded that the radiation has to consist of charged particles. From the measurement of the coincident signal of several particles they deduced that they must have been generated by a single common source, the idea of air showers was born. In air showers, a single primary particle interacts with the constituents of the upper layer of the Earth's atmosphere and produces a cascade of secondary particles.

2.1.1. Cosmic ray flux

Today, the flux of cosmic rays is known over several orders of magnitude in energies up to 10^{21} eV. Since the spectrum is nearly featureless, the ordinate is commonly multiplied by $E^{2.5}$ to pronounce its existing small features, see figure 2.1.

The energy spectrum follows a broken power law

$$\frac{\mathrm{d}N}{\mathrm{d}E} \propto E^{-\gamma} \tag{2.1}$$

where N is the number of primary particles for a given Energy E with a nearly constant power-law index γ.

At low energies below 10^9 eV, the cosmic ray flux is shielded by the magnetic field of the sun and hence correlated to the solar activity. Above 10^{10} eV the influence of the solar activity diminishes and the spectrum follows the power law with $\gamma \approx 2.7$.
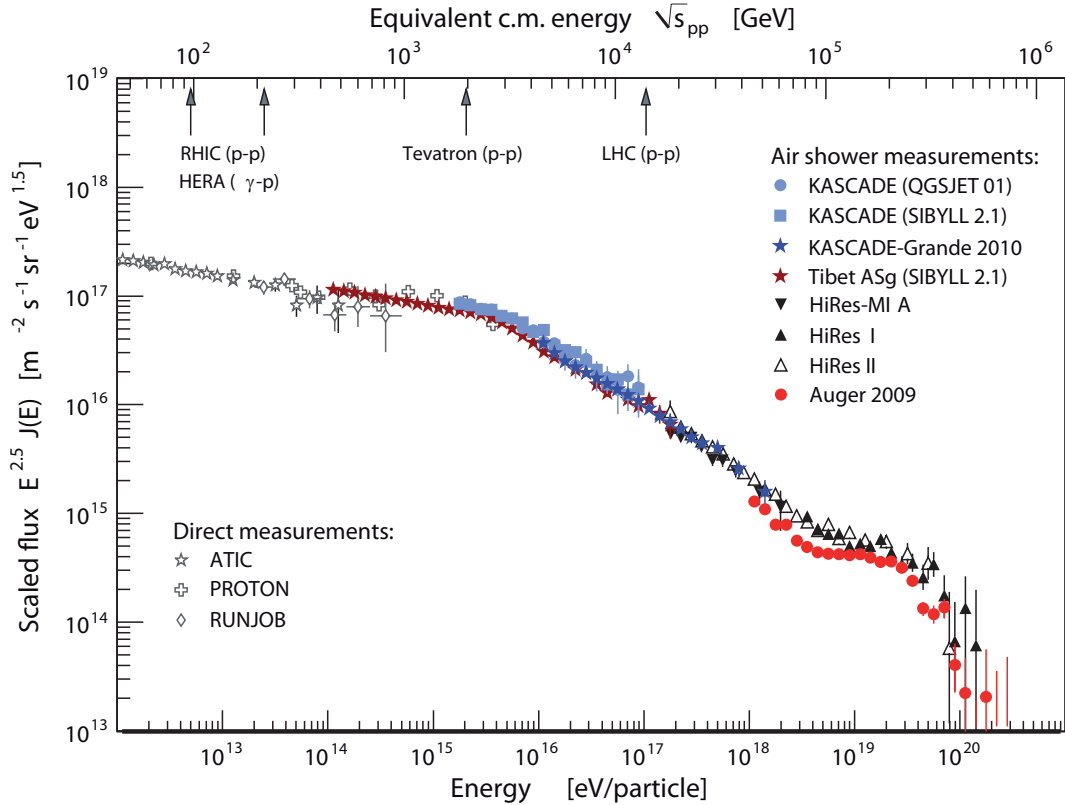
Figure 2.1.: Cosmic ray energy spectrum (taken from [BEH09]). The spectrum shows several distinct features: Around 10^{15} eV, the spectrum gets steeper. At $10^{18.5}$ eV the spectrum flattens again. Above $4 \cdot 10^{19}$ eV, the flux is further of cosmic rays is further suppressed which might be caused by the GZK effect.

However, the spectrum displays a distinct steepening at energies around $E \approx 3 \cdot 10^{15}$ eV which was first observed by Kulikov and Khristiansen in 1956 and is usually called the "knee". The spectral index increases from $\gamma \approx 2.7$ to $\gamma \approx 3.1$. Ever since the knee was discovered there has been an ongoing debate on the origin of this structure. The most accepted explanations are the loss of efficiency of the acceleration mechanism and effects due to the propagation through Galaxy, such as the failing capability of the galactic magnetic field to confine the cosmic rays in the galactic volume [CRE02][BEH09]. Most models predict a change of composition in the knee region. To distinguish between these models, the cosmic ray spectrum has to be measured for different mass groups. One of the main analysis results of the KASCADE experiment at the KIT was the decrease of flux for light elements in the knee region [AAB+05].

Many theories predict a charge dependence of the knee and expect an "iron knee" at about $8 \cdot 10^{16}$ eV [BB07]. First evidence of such a feature has recently been observed by the KASCADE-Grande experiment [AAVB+11].

About an order of magnitude higher in energy at $3 - 4 \cdot 10^{18}$ eV the slope of the spectrum decreases $\Delta\gamma = 0.3 - 0.4$ which is called the "ankle".

In 1966 Greisen, Zatsepin and Kuz'min calculated the energy at which ultrahigh energy hadrons can first interact with the cosmic microwave background [Gre66][ZK66] forming Δ^+ resonances. According to these predictions, the spectrum should steepen around $5 \cdot 10^{19}$ eV as cosmic rays from distant sources suffer energy losses with a mean free path of about 50 Mpc. Heavy particles are broken up due to photodisintegration by cosmic microwave background photons. Recent measurements have indeed shown an increase of the spectral index which is consistent with the GZK effect [Abr08]. It is still to be determined if the observed steepening is caused by the GZK effect or the end of an acceleration mechanism.

At relatively low energies of up to 10^{14} eV, the flux is still high enough to be directly measured by balloon and satellite experiments. The elemental composition obtained by such measurements is in good agreement with the abundance of elements in the solar system with increased occurrence of lighter elements. The source therefore accelerates ordinary surrounding matter. Heavier elements are broken up in a spallation process in galactic matter on their path from the source to Earth [Gru10].

The fading flux at higher energies requires bigger calorimetric area which can neither be provided by balloons nor satellites. As a result, experiments must resort to indirect measurement methods. Indeed, measurements of fluorescence and Cherenkov light produced during shower development in the atmosphere can cover the upper part of the energy spectrum.

The JEM-EUSO projects will provide the testbed for a new generation of fluorescence detectors. By increasing the statistics they will hopefully provide an answer on the nature of origin of cosmic rays.

Since ultra-high energy cosmic rays are not significantly deflected by the galactic magnetic fields [Kro94], JEM-EUSO will answer the question of origin by detecting any anisotropic distribution of cosmic rays.

2.2. Extensive air showers

When a cosmic ray strikes the Earth's atmosphere a shower of billions of secondary particles, an extensive air shower (EAS), is produced. This cascade develops through the whole atmosphere, emitting fluorescence and Cherenkov light. The first interaction occurs typically between 10 to 40 km above the ground and produces daughter particles carrying the energy of the primary particle. These daughter particles further interact, leading to a pancake-like shower front of about 2 m thickness.

An EAS has electromagnetic, hadronic and muonic components. Which of these components takes predominance depends on the type of the primary particle. The hadronic interactions produce mostly π and K mesons. The π^0 decays to photons which again form $e^\pm$ pairs. The electrons form the majority of charged particles in the shower. The $\pi^\pm$ and K mesons further decay into μ and ν which can be directly detected at ground level.
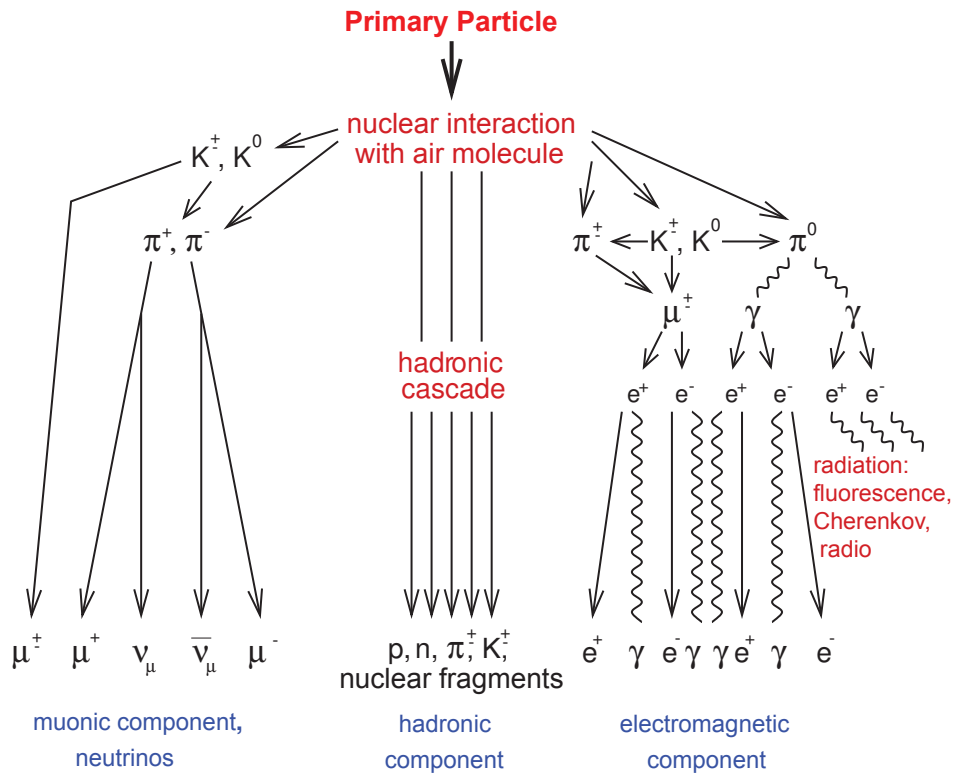
Figure 2.2.: Schematic description of the air shower composition. (Taken from [HRR03])

2.3. Light production

During the development of the shower several types of electromagnetic radiation is emitted. This ranges from radio emissions of coherent pulses in the MHz regime used in the LOPES [Fo05] and AERA [Ber09] to ultraviolet light emissions. This light is emitted by excited nitrogen molecules as the shower dissipates much of its energy by exciting and ionizing air molecules.

2.3.1. Fluorescence light

The secondary particles in the extended air shower (EAS) can excite the air molecules to metastable energy levels. After a short relaxation time, the molecules return to the ground state emitting a characteristic fluorescence light isotropically. The spectral peaks of this light lie in the UV band between 330 nm and 400 nm. There are two major models for fluorescence production.

2.3.1.1. Energy deposit model

The energy deposit model is based on the deposited energy in the atmosphere [ADE$^+$12]. For a distance step dl, one can calculate the photon production as

$$\frac{\mathrm{d}n_{\mathrm{ph,fluo}}^{\mathrm{axis}}(l, \lambda_{\mathrm{fluo}})}{\mathrm{d}l} = \frac{\mathrm{d}E}{\mathrm{d}X}(X_{\mathrm{slant}}) \cdot Y_{\mathrm{fluo}}(T, \rho, \lambda_{\mathrm{fluo}}) \cdot \left(\frac{\mathrm{d}E}{\mathrm{d}X}\right)_0^{-1} \qquad (2.2)$$

where l is the distance from the shower impact location. The measured fluorescence yield Y_{fluo} is given in photons / m for electrons at fixed energy E_0, $(\mathrm{d}E/\mathrm{d}X)_0$ is the normalization constant for electrons of energy E_0.

This model is used in the Auger $\overline{\mathrm{Off}\underline{\mathrm{line}}}$ simulation framework.

2.3.1.2. Number of electrons model

The number of electrons inside a shower step dl can also be used to calculate the number of photons emitted for a given wavelength λ_{fluo} [BBM$^+$09] as

$$\frac{\mathrm{d}n_{ph,\mathrm{Fluo}}(l, \lambda_{\mathrm{fluo}})}{\mathrm{d}l} = N_e \int_E \left(\frac{1}{N_e}\frac{\mathrm{d}N_e}{\mathrm{d}E}\right) \cdot Y_{\mathrm{fluo}}(E, \lambda_{\mathrm{fluo}}, P, T)\, \mathrm{d}E \qquad (2.3)$$

where N_e is the number of electrons above a certain energy level and $\frac{1}{N_e}\frac{\mathrm{d}N_e}{\mathrm{d}E}$ is the normalized energy spectrum. Typically, the energy spectrum is not included in the Monte-Carlo simulation results and only the numbers of electrons N_e are provided. Special care has to be taken to use the correct fluorescence yield since the energy threshold and the way upward going electrons are counted depends on the Monte Carlo simulation.

This model is used in the ESAF simulation framework with a photon yield measured by Nagano at al. [NKSA03] and energy distribution by M. Giller.

2.3.2. Cherenkov light

Numerous secondary particles have velocities greater than the speed of light in the atmosphere. Hence, Cherenkov light is emitted by all charged particles above the Cherenkov emission threshold E_{Ckov}. Since the shower is dominated by electrons, the number of Cherenkov photons per length along the shower axis is by good approximation proportional to the number of electrons [ADE$^+$12]:

$$\frac{\mathrm{d}n_{\mathrm{ph,Ckov}}^{\mathrm{axis}}(l, \lambda_{\mathrm{Ckov}})}{\mathrm{d}l} = Y_{\mathrm{Ckov}}(s, \lambda_{\mathrm{Ckov}}) \cdot N_{\mathrm{Ckov}}^{\mathrm{e}}(X_{\mathrm{slant}}) \qquad (2.4)$$

where Y_{Ckov} is the parameterized total Cherenkov yield for all electrons above E_{Chkov}.

The emission of Cherenkov light is strongly angular dependent and preferably emitted in forward direction of the shower. For a given shower position l one therefore has to consider the Cherenkov light developed earlier. Of cause, the beam is attenuated while propagating

through the atmosphere by Mie and Rayleigh scattering. In its algorithmic form it can be expressed recursively:

$$n_{\text{ph, beam}}^{\text{axis}}(l = 0, \lambda_{\text{Ckov}}) = 0 \tag{2.5}$$

$$n_{\text{ph, beam}}^{\text{axis}}(l, \lambda_{\text{Ckov}}) = \left(\text{d}l \, \frac{\text{d}n_{\text{ph, Ckov}}^{\text{axis}}(l, \lambda_{\text{Ckov}})}{\text{d}l} + n_{\text{ph,beam}}^{\text{axis}}(l - \text{d}l, \lambda_{\text{Ckov}}) \right) \tag{2.6}$$
$$\times \, T_{\text{Mie}} \, T_{\text{Rayleigh}}$$

Additionally the photons can be isotropically diffused when the Cherenkov beam reaches land, sea or clouds. This is commonly referred to as the "Cherenkov echo" and can also be used for reconstruction of the shower direction.

3. The JEM-EUSO telescope

The JEM-EUSO telescope is an optical telescope which detects extended air showers by observing the air fluorescence light. These observations allow the reconstruction of arrival direction and energy of the primary particle. In contrast to ground based observation, space based telescopes can cover huge amounts of atmosphere isotropically which allows better statistics of rare ultra high energy particles and a uniform detection of cosmic rays over the whole celestial sphere.

John Linsley first proposed [Lin79] to observe the Earth's atmosphere from space in 1979. Since then, several projects were proposed and studied, including the *Orbiting Wide-angle Light-collectors* Experiment (OWL) [OWL], KLYPVE/TUS [KAB$^+$04] and several iterations of the *Extreme Universe Space Observatory* (EUSO). The initially planned EUSO observatory, now referred to as ESA-EUSO, was proposed by the European Space Agency (ESA) as a mission attached to the Columbus module of the International Space Station (ISS). In 2004, ESA-EUSO successfully completed the phase A [EUS04] from both technical and scientific point of view. Unfortunatly, ESA-EUSO was put on hold after the Columbia Space Shuttle accident in 2003 because of programmatic issues following the tragic accident. In 2006, the EUSO mission was redefined by the Japan Aerospace Exploration Agency (JAXA) to be attached to the Japanese Experiment Module/Exposure Facility (JEM/EF) aboard the ISS and is now named JEM-EUSO.

The JEM-EUSO telescope is a high-resolution, large-aperture telescope with a wide field of view. The lens system consists of two Fresnel lenses and a high precision diffractive lens. The optics focuses incident UV light onto the focal surface with less than 0.1° special resolution. The focal surface is covered with a rectangular grid of 4932 multi-anode photo-multiplier (MAPMT). Each MAPMT consists of 64 pixels which are registered by electronics equipped with single photon counting ability. The electronics counts photons in 2.5 μs intervals (Gate Time Unit, GTU) and transfers the result to a ring buffer. When an EAS pattern is detected by the trigger algorithms, the shower information is saved and queued for transfer to the ground station.

The effective area observed by the telescope can be further increased by inclining the telescope from its normal nadir orientation (see figure3.1), the so-called "tilted mode". But as the effective area increases, the threshold energy rises because of the growing distance to the air shower and atmospheric attenuation.

Figure 3.1.: JEM-EUSO attached to the Japanese Experimental Module (JEM) in nadir (left) and tilt (right) mode [JEM10].

3.1. Characteristics of space telescopes

Cosmic ray experiments have several characteristics which are commonly used to describe the performance of the experiment, the most important of which shall be briefly described here.

The differential primary particle flux

$$J(E) = \frac{\mathrm{d}\Phi}{\mathrm{d}E\mathrm{d}\Omega} \propto E^{-\gamma} \tag{3.1}$$

follows a power law with a spectral index γ.

A cosmic ray experiment covers an active detection surface S which measures the differential primary particle flux $J(E)$ above an energy threshold of E_{th} over the observed solid angle Ω. Consequently, the expected event rate during data taking is

$$\frac{\mathrm{d}N}{\mathrm{d}t} = \int_S \int_\Omega \int_{E_{\mathrm{th}}}^\infty \mathrm{d}S\mathrm{d}\Omega\mathrm{d}E \, \cos\theta \cdot \epsilon(\vec{x}, \theta, \phi, E) \, J(E) \tag{3.2}$$

where $\epsilon(\vec{x}, \theta, \phi, E)$ represents the detection efficiency. For fluorescence detectors, the detection efficiency ϵ typically increases with energy until the air shower signal can clearly be separated from background noise, after which ϵ becomes constant.

The geometric and effective aperture is defined based on the expected event rate (3.2)

$$\mathcal{A}_{\mathrm{geo}} = \int_S \int_\Omega \mathrm{d}S\mathrm{d}\Omega \cos\theta \tag{3.3}$$

$$\mathcal{A}_{\mathrm{eff}} = \int_S \int_\Omega \mathrm{d}S\mathrm{d}\Omega \cos\theta \cdot \epsilon(\vec{x}, \theta, \phi, E) \tag{3.4}$$

Equation (3.2) can now be written as

$$\frac{\mathrm{d}N}{\mathrm{d}t} = \mathcal{A}_{\mathrm{eff}} \int_{E_{\mathrm{th}}}^\infty \mathrm{d}E \, J(E) \tag{3.5}$$
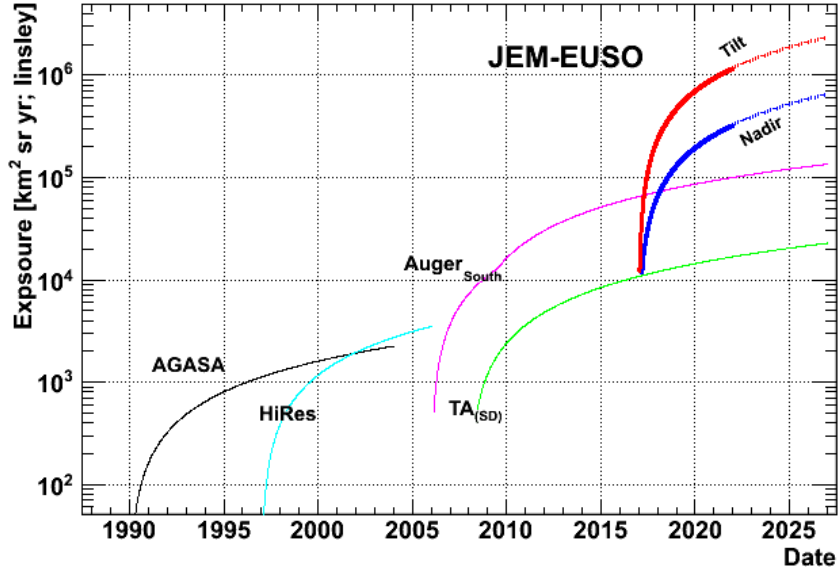
Figure 3.2.: Expected cumulative exposure of JEM-EUSO compared to other cosmic ray experiments. The thick red curve corresponds to tilted mode, the blue curve corresponds to nadir mode.[JEM10]

Since all above expressions have ignored the duty cycle η of the instrument, one can now introduce the exposure Σ of the experiment as

$$N = \int_{\Delta t} \mathrm{d}t\, \eta\, \mathcal{A}_{\mathrm{eff}} \int_{E_{\mathrm{th}}}^{\infty} \mathrm{d}E\, J(E) = \Sigma \int_{E_{\mathrm{th}}}^{\infty} \mathrm{d}E\, J(E) \tag{3.6}$$

where N is the detected number of events over the observation duration Δt.

Naturally, all experiments try to maximize the exposure Σ, since it is directly proportional to the number of detected events. A comparison between the expected exposure of JEM-EUSO and retired and running observatories can be found in figure 3.2.

3.2. Components

From a simulational point of view, the telescope consists of three major functional components (see figure 3.3) which are the collecting optics, the focal surface detector and electronics.

3.2.1. Optics

The optics module of JEM-EUSO is strongly based on the solution found during the phase A study of ESA-EUSO. It is primarily based on two 2.5 m diameter curved doublet Fresnel
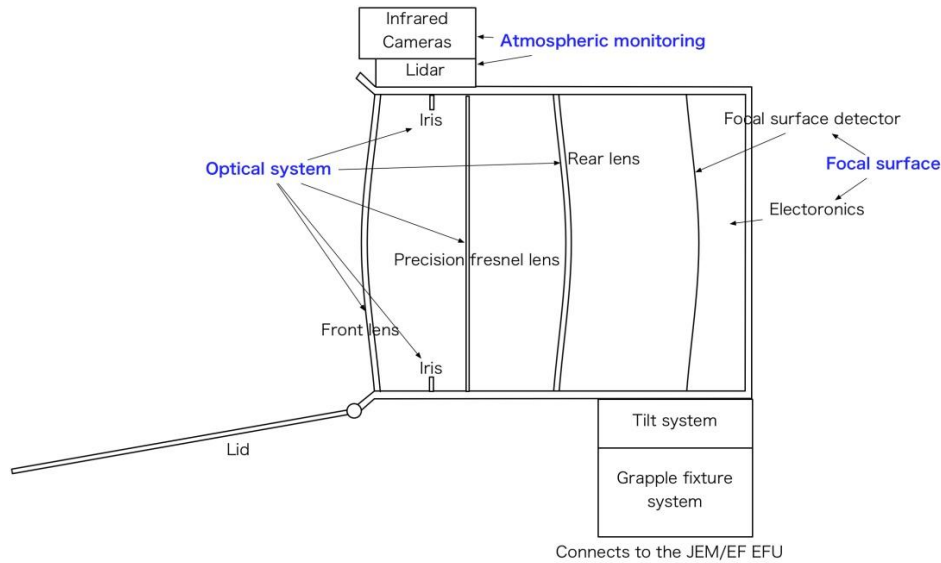
Figure 3.3.: Conceptual design of the JEM-EUSO telescope. [JEM10]

lenses with an intermediate diffractive Fresnel lens to reduce vignetting and correct chromatic aberration. The optics is required to separate the point light emission with a special resolution better than $0.1°$.

Two possible design versions have been proposed which mainly differ in the type of the lens material. The "baseline" design uses polymethyl methacrylate (PMMA) which has proven to be space qualified. The "advanced optics" design uses the fluoropolymer CYTOP for the front and rear Fresnel lenses which has a superior optical performance but no record of usage in space.

3.2.2. Focal surface and electronics

The focal surface (FS) is covered with a curved rectangular grid of 4932 multi-anode photomultiplier (MAPMT). The 2×2 MAPMTs are structured into an "elementary cell" (EC). Nine EC are further arranged in a 3×3 grid forming a "photo detector module" (PDM). The focal surface is a rectangular arrangement of 137 PDMs, which leads to a high resolution of 315 648 Pixels.

The electronics has single photon counting capability which counts individual photons occurring during a gate time window (GTU). This time unit is currently $2.5\,\mu$s and builds the basis of all other electronic clock signals and is also extremely fundamental during simulation.

Since the raw data rate of the high-pixelated sensor will be in the Tbs^{-1} region, the data stream has to be greatly reduced by a cascade of triggers. The simple low-level trigger algorithms are working at PDM level and are filtering for intense, persistent photon counts. Higher level trigger algorithms operate on a cluster of eight PDMs, searching for a linearly moving light trace.
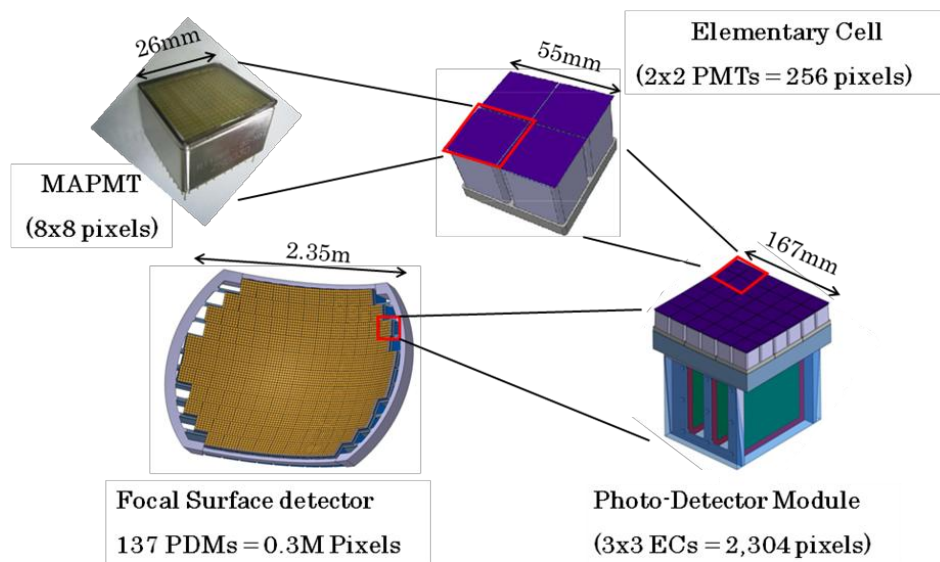
Figure 3.4.: The functional building blocks of the JEM-EUSO focal surface electronics. The basic detector module is a multi-anode photomultiplier (PAPMT) with 8x8 pixels. [JEM10]
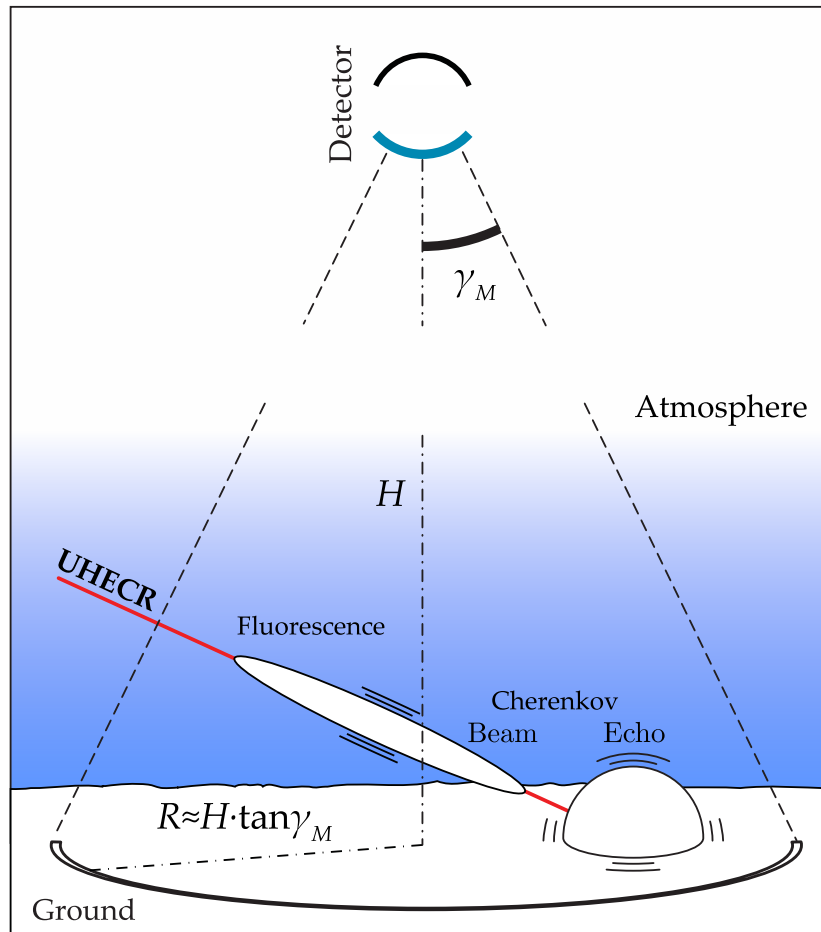
Figure 3.5.: Observation principle for extended air showers from space. γ_M is half the field of view (FOV) angle, H is the detector height and R the projected radius of monitored earth surface. (Adapted from [The06])

4. Simulation frameworks

4.1. Existing simulation frameworks

All modern cosmic ray experiments are demanding large-scale research experiments which require monetary and long term commitment. It is therefore necessary to have a sound simulation and analysis framework.

The simulation of such air shower experiments naturally starts with the description of the shower development in the atmosphere. This is either a parametrized description or calculated by external simulation programs. The most well known programs are CORSIKA [HKC$^+$98] and CONEX [BEH$^+$07]. CORSIKA does a full Monte Carlo simulation of the shower development which requires massive computational power. This thesis mostly facilitates CONEX which is a 1D hybrid simulation. It calculates a full MC simulation for the first few leading high energy interactions and falls back to a parametrized description of the shower development for lower energies.

Typically, each experiment has its own software framework for simulation and analysis. The Pierre Auger Collaboration has developed a versatile and powerful software framework called $\overline{\text{Off}}\underline{\text{line}}$ [ABG$^+$07].

On the other hand, there exist two separate simulation projects for JEM-EUSO. The older program is called the "**EUSO S**imulation and **A**nalysis **F**ramework" (ESAF) and was written during the Phase A study of ESA-EUSO in 2003. When JAXA revived the JEM-EUSO project, they also developed their own simulation program, the so called "Saitama code" (STM) which is only used internally by JAXA.

The $\overline{\text{Off}}\underline{\text{line}}$ and ESAF frameworks both aim to provide an end-to-end simulation. This means that they will simulate light production and light propagation through the atmosphere to the telescope followed by optics simulation. In addition, they will also do electronics simulation, starting with the photoelectron production in the PMTs, electronics and triggering algorithms. Both simulation frameworks also support the reconstruction and analysis of the simulated data, which is not investigated by this thesis.

4.2. The Auger $\overline{\text{Off}}\underline{\text{line}}$ Framework

4.2.1. Overview

The Auger $\overline{\text{Off}}\underline{\text{line}}$ framework [ABG$^+$07] is written in C++ and takes advantage of object oriented design and common open source tools such as *make*, *unittest* and the *boost libraries*.

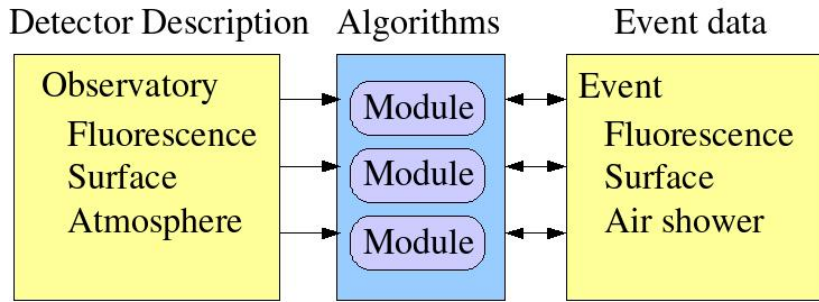Figure 4.1.: General structure of $\overline{\text{Off}}\underline{\text{line}}$ from an algorithmic perspective. All simulation tasks are broken down to modules which operate on the detector description and event data. Information is exchanged via the event data and is not passed in specialized interfaces between the modules. Due to this design modules do only rely on the availability of data in event data and are not strongly entangled with each other. (Figure taken from [ABG⁺07])

All physical processes are encapsulated in separate modules which can easily be exchanged. The configuration of module parameters is done over XML files which are checked with W3C XML Schema validation. A user can easily chain several modules together with sequencing files which are interpreted by a *run controller*, enabling different simulation chains without any recompilation. Modules operate on an event data structure and static detector descriptions. Because they only modify or add data in the defined event data interface there is no strong dependence between the different modules. The user only has to chain the modules in the right order so that the data is available once it is required by a module.

Aside from physics, $\overline{\text{Off}}\underline{\text{line}}$ does also provide utility functions, including a versatile geometry package. Because of the size of the experiment the curvature of the earth cannot be neglected. $\overline{\text{Off}}\underline{\text{line}}$ therefore provides methods to manipulate abstract geometrical objects independently of the coordinate system. Moreover, the basic coordinate systems in $\overline{\text{Off}}\underline{\text{line}}$ are based on the WGS[1] 84 ellipsoid.

Auger $\overline{\text{Off}}\underline{\text{line}}$ has been in constant development since 2003 which has resulted in generally good code quality and a majored physics simulation. In addition, because $\overline{\text{Off}}\underline{\text{line}}$ has been developed for a running experiment, it has constantly been verified with true experimental data.

4.2.2. Default $\overline{\text{Off}}\underline{\text{line}}$ fluorescence simulation chain

As described in the previous paragraph, modules can be chained together by the user to form a simulation chain which is interpreted by the *run controller*. It lies in the responsibility of the user to chain the modules in the right order so that each module can rely on data which has been generated by the previous module. Of course, the simulation chain is very specific to which aspect of the extensive air shower shall be simulated.

---

[1]World Geodetic System

16

```
1  <module> EventFileReaderOG              </module>
   <module> GeometryGeneratorKG            </module>
3  <module> EventGeneratorOG               </module>

5  <module> ShowerLightSimulatorKG         </module>
   <module> LightAtDiaphragmSimulatorKG    </module>
7  <module> ShowerPhotonGeneratorOG        </module>

9  <module> TelescopeSimulatorKG           </module>

11 <module> FdBackgroundSimulatorOG        </module>
   <module> FdElectronicsSimulatorOG       </module>
13 <module> FdTriggerSimulatorOG           </module>

15 <module> EventFileExporterOG            </module>
```

Listing 4.1: Simple fluorescence simulation chain for Auger telescopes. The OG and KG suffix denotes which Auger group has developed the module.

Program listing 4.1 shows a typical simulation chain used for florescence detection (FD) simulation. The simulation chain consists of several independent steps:

Event generation The shower profile is read from files by *EventFileReaderOG*. *EventFileReaderOG* can handle several types of input formats, the most important of which are CONEX and CORSIKA files. As the shower profile has no absolute impact location it is placed by *GeometryGeneratorKG* and *EventGeneratorOG* relative to telescopes or at a fixed location.

Light generation The *ShowerLightSimulatorKG* module does calculate the number of photons generated by the shower. The light is propagated through the atmosphere by the *LightAtDiaphragmSimulatorKG* module. Once the amount of incident light is calculated, the *ShowerPhotonGeneratorOG* places bundles of photons over the optics entrance.

Telescope simulation Once the photons on the entrance of the optics have been calculated they are ray traced through the Auger telescope by *TelescopeSimulatorKG*. Finally, the response of the PMTs and electronics is simulated and the result is saved in a ROOT file.

The telescope simulation modules form the natural border between shower and atmosphere physics and the specific telescope. When interfacing ESAF to $\overline{Off\underline{line}}$ a new module replaces the telescope simulation and takes care to translate the $\overline{Off\underline{line}}$ objects to ESAF.
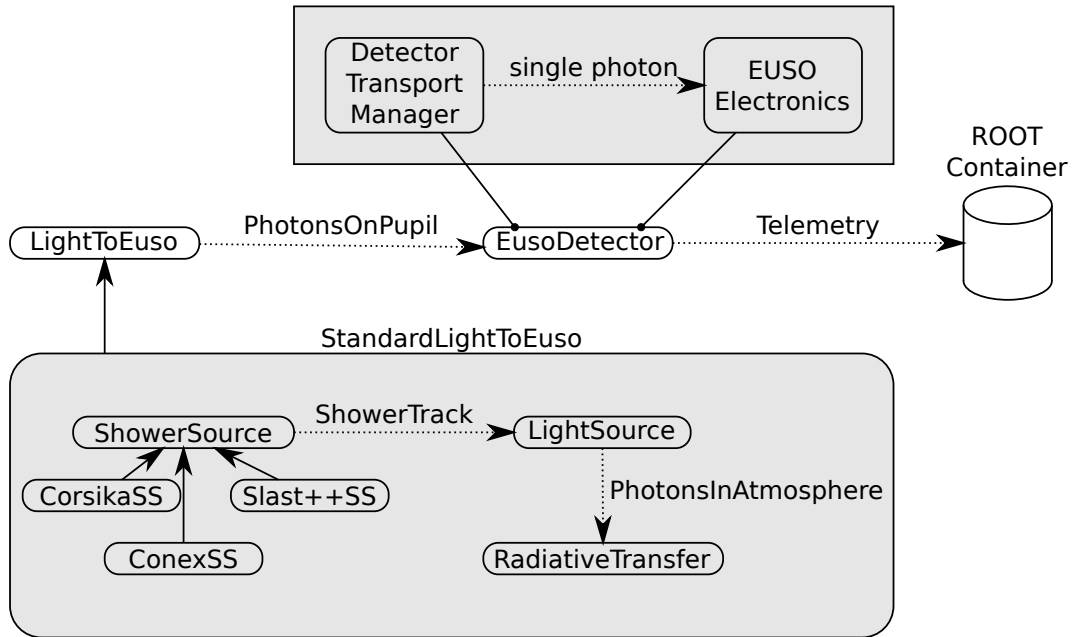
Figure 4.2.: Simplified standard ESAF simulation chain. The interface between shower
physics and detector is the PhotonsOnPupil object passed between *LightToEuso*
and *EusoDetector*. The *StandardLightToEuso* class allows multiple types of shower
descriptions, including CONEX and CORSIKA. The *StandardLightToEuso* can be
replaced by *PhPRootFileLightToEuso* which will read PhotonsOnPupil objects di-
rectly from a ROOT file.

4.3. ESAF

The *E*USO *S*imulation & *A*nalysis *F*ramework (ESAF)[BBM+09] was developed during the
phase A study by the ESA in 2003. It is mostly written in C++ and also uses object oriented
design patterns.

All important physical processes are divided into class modules with abstract interfaces
for each physical process. In contrast to $\overline{\text{Off}\underline{\text{line}}}$, ESAF modules do not operate on shared
event data but rather pass data between the different module interfaces. As a result ESAF
modules are strongly entangled with each other and do not allow easy chaining of modules.

Since ESAF has been developed in respect to a single telescope experiment it cannot sim-
ulate several telescopes at the same time. This makes the simulation of stereo shower
observation impossible with the current code.

4.3.1. ESAF simulation chains

The ESAF simulation chain is based on two abstract classes called *LightToEuso* and *EusoDe-
tector*, see figure 4.2. All physics outside the telescope is described by *LightToEuso*. The
class is responsible for passing all photons at the pupil of the telescope to the *EusoDetec-*

tor class. Several classes inherit from the abstract *LightToEuso* interface, notably the *StandardLightToEuso* and the *PhPRootFileLightToEuso* classes. *StandardLightToEuso* uses a generic *ShowerSource* object which allows several sources of shower description. Typically, a parameterization of shower development is used, the "Shower Light Attenuated to the Space Telescope in C++" generator (SLAST++). This class is called *SlastShowerSource* and is the only actively maintained shower generator.

In addition to the *SlastShowerSource* there is also a CONEX file reader. During this thesis, the CONEX file reader module has been updated to read the output files produced by recent CONEX versions and multiple severe bugs have been discovered in the *ConexShowerSource* code[2]. Currently the results of the CONEX module cannot be trusted and are presented for comparison only.

The whole shower and atmosphere simulation can also be circumvented with the *PhPRootFileLightToEuso* module which replaces the *StandardLightToEuso* module. The *PhPRootFileLightToEuso* module will only read photons from a ROOT container file and pass it directly to *EusoDetector*. In this thesis, the *PhPRootFileLightToEuso* module will be used to pass the Offline simulation results to ESAF.

4.3.2. ESAF ROOT container

All ESAF ROOT output files such as the *PhotonOnPupil* use special output container classes which partially mirror the functionality of the classes used during the computation. The container classes all begin with the capital letter E, i.e. the internal class *Photon* maps to the *EPhoton* class in saved ROOT files.

Unfortunately, there is no converter between internal and external ROOT container classes which requires manual mapping of the member attributes to the container attributes and vice versa. Additionally, the class interface might differ between the two classes.

---

[2]Commit #2982 fixes missing time information. Before the commit the shower was simulated backwards but Cherenkov light was simulated in forward direction.

5. Offline to ESAF interface module

5.1. Introduction

While working on this thesis an interface between $\overline{\text{Off}}\underline{\text{line}}$ and ESAF has been developed. The design goal of this interface was to leave all common physical processes in the $\overline{\text{Off}}\underline{\text{line}}$ simulation and use ESAF for the telescope description. The natural border between the atmosphere and the detector is the entrance pupil of the optics. This interface therefore uses $\overline{\text{Off}}\underline{\text{line}}$ to simulate the shower light production and propagation to the telescope up to the entrance of the pupil. The photons are then saved inside a ROOT container file which can easily be read by all ESAF versions since 2005.

There are several unique advantages of using $\overline{\text{Off}}\underline{\text{line}}$ as the base simulation framework. Most notably, the simulation has been constantly verified with data from the Pierre Auger Telescope. Since simulation and interpretation of air shower experiments strongly depend on the models used for the high energy interactions during shower development it is advantageous to have well working interfaces to shower simulators such as CORSIKA[HKC$^+$98] and CONEX[BEH$^+$07]. Because $\overline{\text{Off}}\underline{\text{line}}$ has been developed for the Pierre Auger Observatory which uses multiple fluorescence telescopes, $\overline{\text{Off}}\underline{\text{line}}$ is well suited to simulated multiples space telescopes in arbitrary rotations such as the stereo satellite OWL experiment and earthbound JEM-EUSO prototypes.

Because of the modular design of $\overline{\text{Off}}\underline{\text{line}}$ it is relatively easy to include a new interface module in the simulation chain. Consequently, all important code changes have been made to the Offline core and a new Offline module. Great care has been taken to adopt the existing Auger detector description to the JEM-EUSO experiment. The adapted configuration includes changes to the field of view, geometric orientation and shower parameters.

Unfortunately, the ESAF ROOT container used to transfer data between $\overline{\text{Off}}\underline{\text{line}}$ and ESAF does only contain information about the propagated photons at the telescope pupil and basic information about the simulated shower. The interface module is hence only meant as a first proof-of-concept and does not claim to be a complete solution to interface Auger $\overline{\text{Off}}\underline{\text{line}}$ to ESAF.

5.2. Technical description

The interface module has been developed as an independent module for the Auger $\overline{\text{Off}}\underline{\text{line}}$ Framework. It is contained in a collection of additional $\overline{\text{Off}}\underline{\text{line}}$ modules called *OfflineKG*
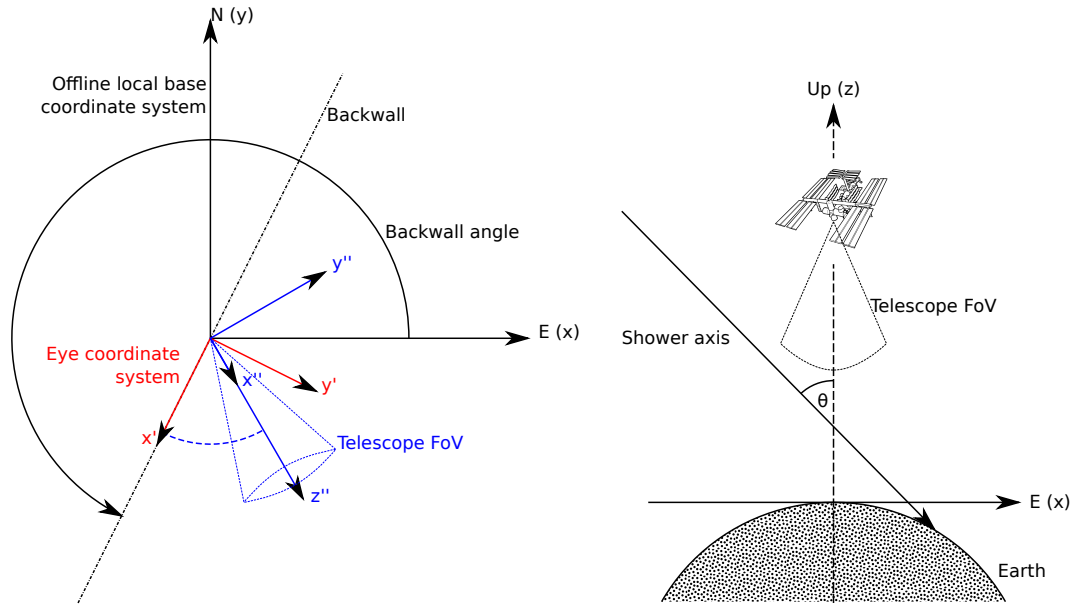
(a) Top-down projection of relevant Offline coordinate systems. The base coordinate system (black) is a local east, north, up coordinate system. The eye coordinate system (red) is a rotated base coordinate system and origin of all derived telescope systems (blue). The telescope system has the z-axis pointing in direction of the optical axis, therefore pointing outside of the projection plane.

(b) The ESAF base coordinate system is a local East, North, Up coordinate system defined directly below the satellite (nadir position). Incoming showers are described in this coordinate system and not at impact location.

Figure 5.1.: Important coordinate systems in $\overline{\text{Off}}\underline{\text{line}}$ and ESAF.

which is hosted by the KIT. The module can be inserted into a normal $\overline{\text{Off}}\underline{\text{line}}$ fluorescence simulation chain instead of, or in parallel to the normal Pierre Auger Observatory telescopes.

The module exports all photons at the optics of a specified telescope into a ROOT container which can be read via the ESAF *PhPRootFileLightToEuso* module.

Apart from just inserting the interface module in the simulation sequence, extensive changes to the Auger detector setup configuration are necessary to add JEM-EUSO to the list of telescopes. The supplemental configuration files are provided in the *OfflineKG* examples.

5.3. Coordinate systems

One of the major aspects of exchanging data between ESAF and $\overline{\text{Off}}\underline{\text{line}}$ is to account for all coordinate systems and their transformation. The following chapter will therefore take a detailed look at all relevant coordinate systems.

5.3.1. ESAF

Unfortunately, there is no dedicated documentation of the ESAF coordinate systems. All information regarding the ESAF coordinate system handling has been directly extracted from the source code and private communication with the head ESAF developer Dmitry Naumov.

The ESAF base coordinate system, called *M*aster *E*SAF *S*ystem (MES), is an East, North, Up coordinate system defined at earth level at nadir position below the satellite, see figure 5.1a on the facing page.

The ESAF optics coordinate system has the same orientation as the ESAF base coordinate system but the origin coincidences with the center of the detector.

For tilt mode, you can specify a rotation matrix which will transform the tilt geometry coordinates to the ESAF base coordinate system. Unfortunately, these rotations are disabled by default and not supported by the SLAST++ shower generator and parts of the reconstruction framework.

5.3.2. Offline

Because the Pierre Auger Observatory consists of several telescopes which are distributed over a large area there is no distinct main coordinate system. Instead, $\overline{\text{Off}}\underline{\text{line}}$ provides strong support for multiple coordinate systems with reference points. There are vectors and points which are implemented as abstract geometric objects in space which can easily be represented in any coordinate system of choice. The default local coordinate system orientation is an East, North, Up coordinate system in any freely defined point of origin.

Eye coordinate system   Because Offline has been developed for the Pierre Auger Observatory, it supports several telescopes to be grouped together to one "eye" which share a common location but different viewing angles. Together, all telescopes cover 180° of view and are placed against a concrete "backwall". The eye coordinate system is derived from the base coordinate system at the eye location by rotating around the z axis by the backwall angle. This will give a coordinate system with the x-axis parallel to the backwall and z-axis pointing up.

Telescope coordinate system   Each telescope has an elevation and azimuth angle which describe the telescope pointing direction as spherical coordinates in the eye coordinate system. The telescope coordinate system is oriented according to the telescope pointing direction with the z-axis pointing away from the telescope and parallel to the optical axis. The y-axis is parallel to ground, and the x axis is orthogonal to ground level.

JEM-EUSO in Offline   In the provided Offline JEM-EUSO configuration example, the backwall and azimuth angles are set to zero and the elevation angle is set to $-90\,°$. This

will result in the telescope pointing in nadir direction, with a West, North, Down coordinate system.

Conversion to ESAF main coordinate system   ESAF expects the optical axis to point into the telescope, the z-axis must hence be inverted. To convert the Offline telescope coordinates back to ESAF coordinate systems, the telescope coordinate system is rotated by $180°$ around the y-axis, basically yielding the ESAF east, north, up coordinate system for nadir direction.

For tilt geometries, the interface module will calculate the Euler angles which describe the rotated Offline telescope coordinate system in respect to the ESAF main coordinate system and pass it to ESAF inside the ROOT container.

5.3.2.1. Faked telescope to MES coordinate system

Even though ESAF has initially been designed to handle tilted geometries by transforming between telescope coordinate system and MES system some parts of ESAF don't take these transformations into account. To overcome such limitations, the interface module does allow to export the *PhotonsOnPupil* file as if the telescope were in nadir position (MES system). This mode can be useful to simulate the detector response even though ESAF might normally not be able to handle such an orientation.

5.4. Shower description

Another key difference between Offline and ESAF is the description of shower geometry. ESAF uses spherical coordinates in the ESAF base coordinate system to describe the shower arrival direction (see figure 5.1b). In contrast, Offline uses a local coordinate system at the impact location. The zenith angle definition of ESAF and Offline does therefore differ the further away the impact location is placed from nadir position. At direct nadir impact location is equal to the zenith definition.

The interface module will transform the shower definition to ESAF angles and also save it to the *PhotonsOnPupil* ROOT container. As a result, if one wants to compare showers between Offline and ESAF, the impact location must either be directly below JEM-EUSO or the right angles provided by the interface module have to be used.

5.5. Photon representation

Since the telescopes of the Pierre Auger Observatory are located at ground level they are a lot closer to the shower when it develops in the atmosphere. As a result, the telescope will see a high flux of shower photons. In order to reduce the computational time in $\overline{\text{Off}}\underline{\text{line}}$,

several photons bunches are grouped to *weighted photons*. Each *weighted photon* carries a rational number weight

$$w = i + p \quad i \in \mathbb{Z}_0, \ p \in \{0 \le x \le 1, x \in \mathbb{R}\} \tag{5.1}$$

where the integer part *i* represents the number of true photons in the bunch. The rational part *p* of the weight represents the probability of one further photon in the bunch.

In ESAF, photon bunches are only used for atmospheric propagation but not in optics and electronics simulation. The interface module most therefore convert $\overline{\text{Off}\underline{\text{line}}}$ photons to ESAF photons, taking their weight into account. If the weight is greater one, it is possible that the same photon has to be added several times to the *PhotonOnPupil* file. This might result in a systematic error when simulated with ESAF, as multiple photons will hit the exactly same MAPMT pixel at the same time. To overcome such problems, it is possible to oversample the diaphragm surface with *weighted photons*. Consequently, there will be more *weighted photons* than true physical photons on the diaphragm and *w* is smaller than one, resulting in no duplication of photons. The interface module attempts to detect if such a problem occurs and will warn the user if the photon weight *w* is excessively high.

6. Offline/ESAF simulation result comparison

6.1. Introduction

In addition to implementing the export module, a small comparison between $\overline{\text{Off}\underline{\text{line}}}$ and ESAF based shower simulations was conducted. Since the impact direction parametrization is not equal between $\overline{\text{Off}\underline{\text{line}}}$ and ESAF (see section 5.4), all simulated showers have their impact point directly nadir below JEM-EUSO on sea level for the sake of simplicity.

All showers were generated with the default configuration of $\overline{\text{Off}\underline{\text{line}}}$ and ESAF if not otherwise stated. The $\overline{\text{Off}\underline{\text{line}}}$ simulations are all based on a CONEX shower simulation. In some the photon count comparison, these CONEX files were also directly imported with the ESAF CONEX input module and are presented for reference only.

6.2. Focal surface

The imaged shower on the focal surface provides an intuitive way to get a first impression of the differences between the two simulation paths. Figure 6.1 on the next page displays a proton shower with a primary energy of $E = 10^{20}$ eV and an inclined arrival direction of $\theta = 79°$, $\phi = 30°$. Both simulations were conducted with the default set of parameters of ESAF and $\overline{\text{Off}\underline{\text{line}}}$.

The primary difference between the two simulations lies in the treatment of the Cherenkov light distribution. By default, ESAF ignores the angular distribution of the electrons inside the shower and therefore produces a tightly focused Cherenkov beam which is clearly visible in the upper right half of figure 6.1a. By contrast, $\overline{\text{Off}\underline{\text{line}}}$ uses a parametrization of the lateral distribution of Cherenkov light developed by Gora et al. [GEH+06].

To further compare the effects of Cherenkov light distribution the lateral distribution can be enabled in ESAF. The angular distribution of electrons is based on measurements performed by Fly's Eye detector in 1987 [BCC+87]. Alternatively, the lateral distribution of Cherenkov light can be disabled in $\overline{\text{Off}\underline{\text{line}}}$. Exemplary results of the focal surfaces are provided in the appendix in section A.2.2 and show a good level of agreement.
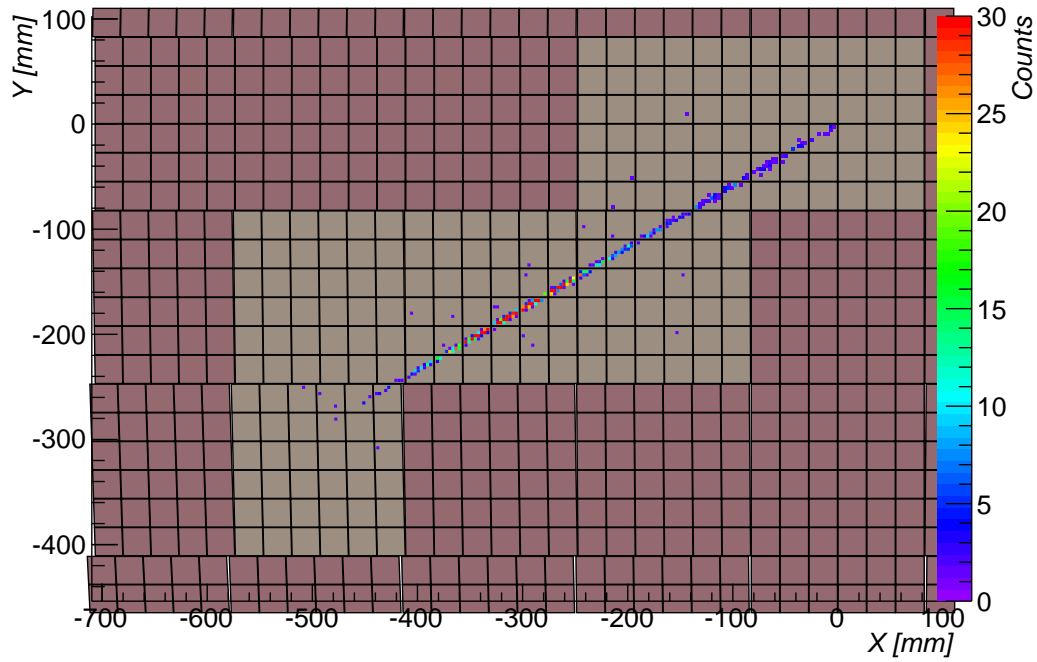
(a) SLAST++ generated shower with default configuration.
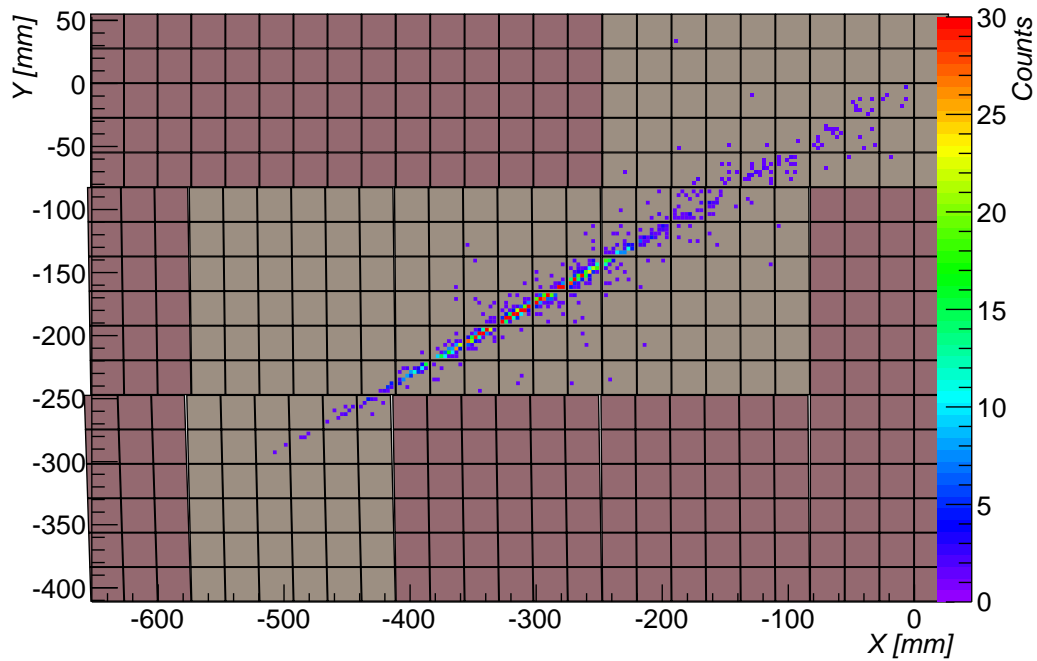
(b) $\overline{\text{Off}\underline{\text{line}}}$ generated shower with default configuration.

Figure 6.1.: Comparison between $\overline{\text{Off}\underline{\text{line}}}$ and ESAF based shower simulation ($E = 10^{20}$ eV, $\theta = 79°$, $\phi = 30°$, proton). The impact point of the shower is located nadir on sea level and hence at $(0, 0)$ mm in the optics. The shower was rotated in the azimuth plane ϕ to avoid systematic effects on the photon count by the PMT lattice. The $\overline{\text{Off}\underline{\text{line}}}$ shower displays a much wider lateral distribution than ESAF, which is primarily caused by ESAF neglecting the lateral distribution of the Cherenkov light by default.
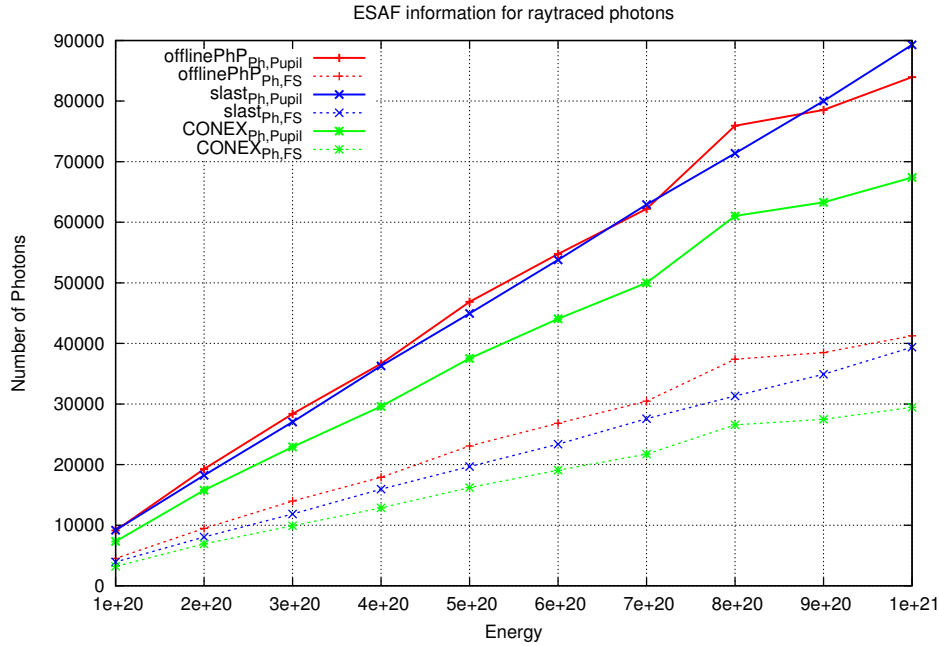
Figure 6.2.: Number of photons at the pupil entrance and on the focal surface after ray-tracing. The shower was always simulated with the same parameters ($\theta = 60°$, $\phi = 30°$, proton) but with energies between $10^{20} - 10^{21}$ eV. The $\overline{\text{Off}\underline{\text{line}}}$ simulation (red) is based on a CONEX shower which is also read in directly with ESAF (green). The ESAF simulation (blue) is based on the default SLAST++ parametrized shower generator with the same parameters as the CONEX shower. Because CONEX is a MC simulation and only one simulation has been conducted per energy, the plot shows some fluctuations at $8 \cdot 10^{20}$ eV.

6.3. Total photon count

The agreement between the different simulation paths can further be compared by changing only one parameter, i.e. energy or zenith angle, and holding all other parameters fixed. A good observable is the total number of photons which reach the entrance of the pupil and the focal surface after ray-tracing.

Since this $\overline{\text{Off}\underline{\text{line}}}$ simulation uses the Monte Carlo CONEX simulation for the simulation of the shower development it shows some fluctuations in the photon counts which are not visible in the pure ESAF SLAST++ simulation, which uses a parameterized shower model.

6.3.1. Energy scan

The total number of photons for a shower with fixed geometry and varying primary energy is depicted in figure 6.2. The deposited energy in the atmosphere increases linearly with the energy of the primary particle which is also reflected in the plot.
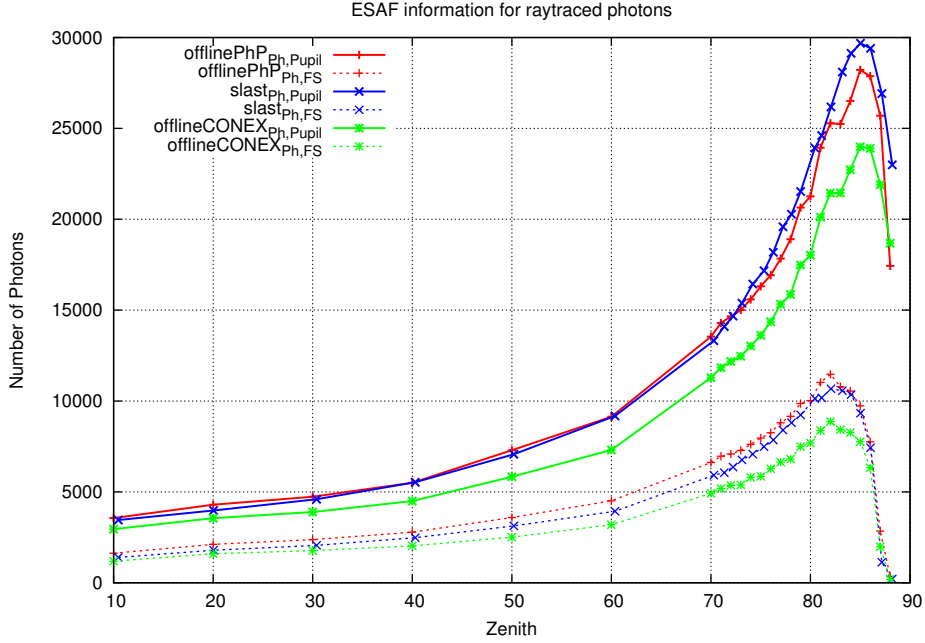
Figure 6.3.: Number of photons at the pupil entrance and on the focal surface after ray-tracing. The shower was always simulated with the same parameters ($E = 10^{20}$ eV, $\phi = 30°$, proton) but with zenith angles between $\theta = 0° - 90°$. The $\overline{\text{Off}\underline{\text{line}}}$ simulation (red) is based on a CONEX shower which is also read in directly with ESAF (green). The ESAF simulation (blue) is based on the default SLAST++ parametrized shower generator with the same parameters as the CONEX shower.

6.3.2. Zenith scan

The impact angle has a huge impact on the observable number of photons from JEM-EUSO. Inclined showers develop higher in the atmosphere and the attenuation of the fluorescence light is consequently decreased due to the reduced atmosphere between the telescope and the shower.

Figure 6.3 shows the increase of photons at the pupil with increasing inclination angle up to $85°$. The increase is followed by a sudden decrease in photons which is caused by the shower developing outside of the JEM-EUSO field of view.

The presence of this decrease at a virtually identical zenith angle is a good indicator for matching detector geometries in all three simulations.

7. Summary and Outlook

The JEM-EUSO project will provide the opportunity to increase the statistics of cosmic ray experiments in the ultra-high energy domain. A strong simulation and reconstruction framework is needed to predict the performance of such an instrument.

In this thesis it was demonstrated that Pierre Auger $\overline{\text{Off}}\underline{\text{line}}$ can be used to simulate fluorescence satellite experiments, such as JEM-EUSO. In addition, a new software module for $\overline{\text{Off}}\underline{\text{line}}$ was developed which exports simulated showers and propagated photons to a ROOT container file which can be read by the ESAF framework. A comparison between the obtained results shows a high level of agreement between both simulations.

Currently, two earthbound prototype projects of JEM-EUSO are under development and are expected to be completed in a two-year time frame. Both prototypes consist of only one PDM board with an adapted JEM-EUSO optic. The EUSO-TA prototype will be located at the Telescope Array in Utah, USA. In contrast to this ground level experiment, the planned EUSO-BA will be a weather balloon experiment.

Since $\overline{\text{Off}}\underline{\text{line}}$ has been developed for ground based telescopes, it is a perfect candidate to simulate ground based and low-altitude prototypes of JEM-EUSO, such as the planned EUSO-TA and EUSO-Ballon projects. With the current state of development the adapter module can already be used to simulate a fictive JEM-EUSO located directly at the Los Leones station of the Pierre Auger Observatory, see figure A.2.

The work on this thesis provided a unique view inside two complex fluorescence simulation frameworks. Simulating all aspects of such an experiment is a difficult task which requires an enormous amount of work. In the same way as air shower simulations are done by specific programs such as CONEX and CORSIKA, it seems logical that a consolidation of the existing fluorescence simulation frameworks is needed. It is the hope of the author that the $\overline{\text{Off}}\underline{\text{line}}$ framework will be the future base of such a software.

A. Appendix

A.1. Interface module Flow chart
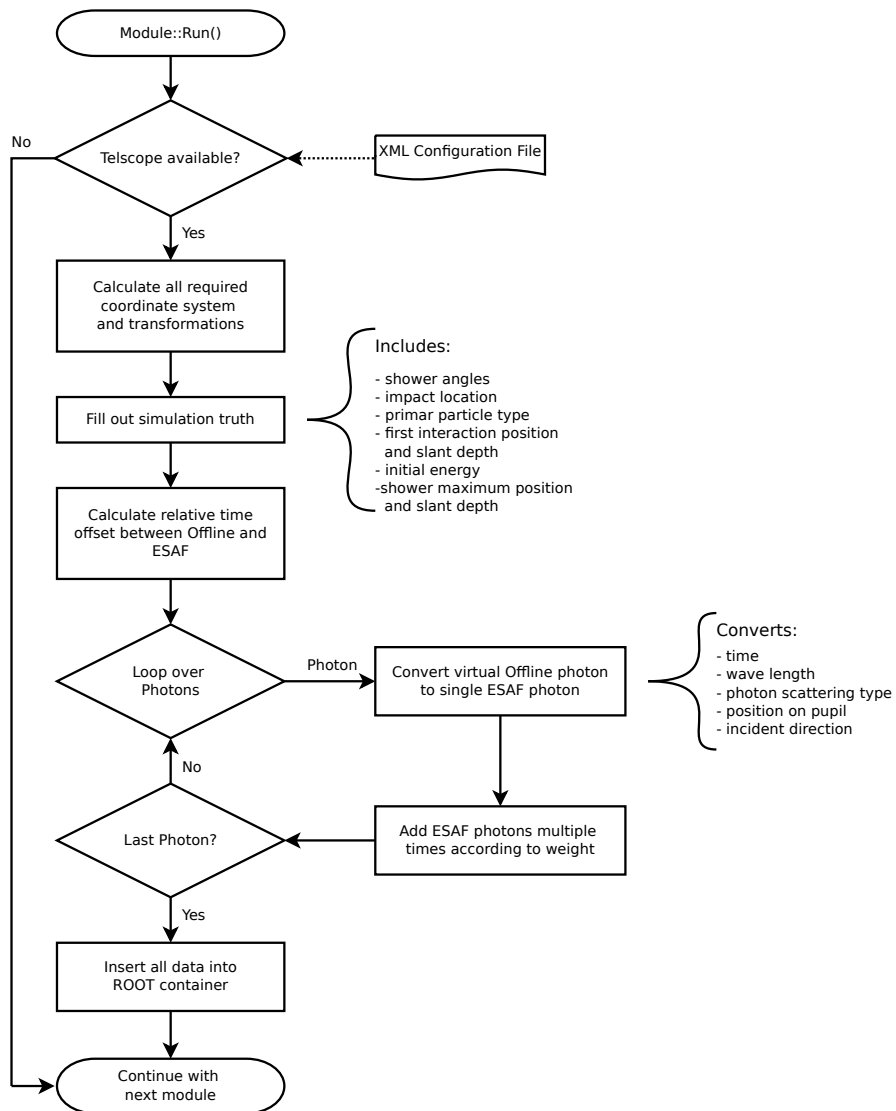
Figure A.1.: Simplified flow chart of the $\overline{\text{Off}\underline{\text{line}}}$ to ESAF interface module. The *Run()* method is called by the *run controller* when the simulation reaches the module in the simulation sequence. Major steps are the coordinate system calculation, conversion of the simulation truth and conversion of $\overline{\text{Off}\underline{\text{line}}}$ photons to the ESAF representation.

The $\overline{\text{Off}\underline{\text{line}}}$ framework allows to easily insert user modules into the simulation chain. A new module was developed for this thesis to interface the shower simulation the telescope simulation in ESAF. Figure A.1 shows the most important conversion steps necessary to produce ROOT output files which can be read by ESAF.

A.2. Focal surface plots

The Focal Surface is the detector surface of JEM-EUSO and is comparable with the optical sensor in a digital camera. Plotting the counted photons on the Focal Surface gives a direct impression of what the telescope is seeing. These plots show the integrated number of detected MC photons over the whole simulation time. Electrical noise of the sensor is not shown in the plots.
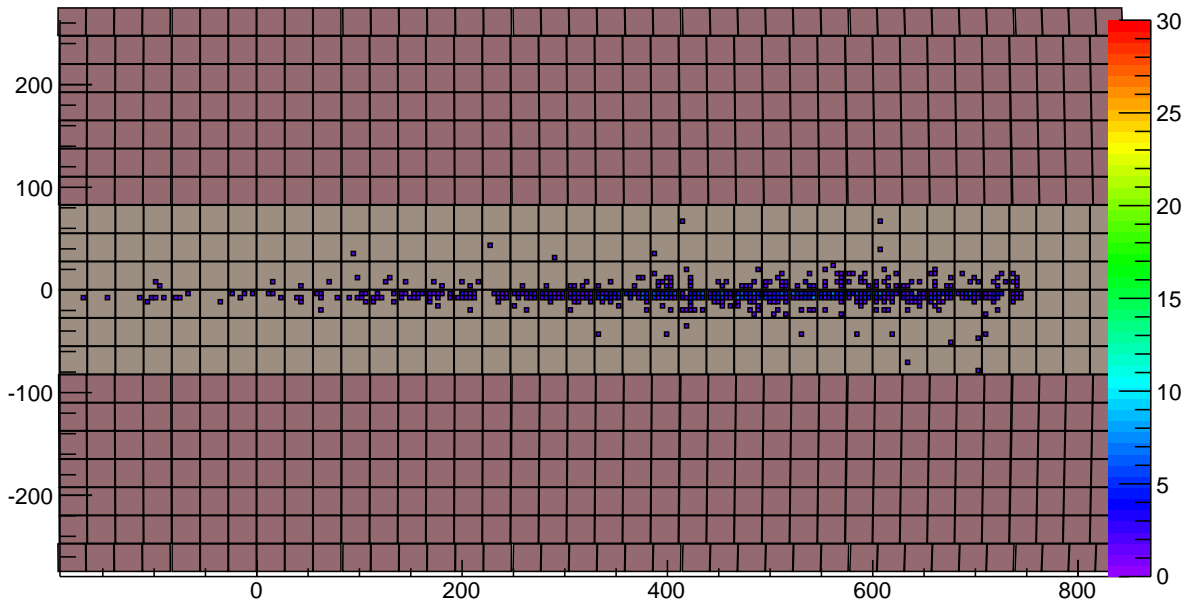
A.2.1. Ground based JEM-EUSO

Figure A.2.: $\overline{\text{Off}\underline{\text{line}}}$ based simulation of a fictive JEM-EUSO located at the Pierre Auger Observatory looking skyward with an elevation of $15°$ at a $E = 10^{20}$ eV, $\theta = 90°$ shower in 30 km distance. The y-axis of the focal surface is parallel to ground level; the negative x-axis is skyward.

The Auger $\overline{\text{Off}\underline{\text{line}}}$ framework provides the ability to simulate a telescope at any location with an arbitrary orientation. This will be extremely useful to simulate planned ground based JEM-EUSO prototypes such as the EUSO-TA, located at the Telescope Array in Utah, USA or for weather balloon experiments such as EUSO-Balloon.

A. Appendix

To demonstrate the flexibility of the $\overline{\text{Off}\underline{\text{line}}}$ framework and the adapter module, the full JEM-EUSO telescope has been shifted to the same location and upward orientation as the center telescope at the Los Leones station of the Pierre Auger Observatory, see figure A.2.

A.2.2. Effects of electron angular distribution

The main discrepancy between $\overline{\text{Off}\underline{\text{line}}}$ and ESAF simulation in their default configuration is the treatment of the Cherenkov emission (compare section 6.2). Fortunately, the behavior of $\overline{\text{Off}\underline{\text{line}}}$ and ESAF can be changed so that the missing Cherenkov lateral distribution of ESAF can be compared with $\overline{\text{Off}\underline{\text{line}}}$ and vice versa.

Once the simulation of the lateral distribution is changed, the results (figure A.3) agree well with the corresponding default simulations (figure 6.1) .
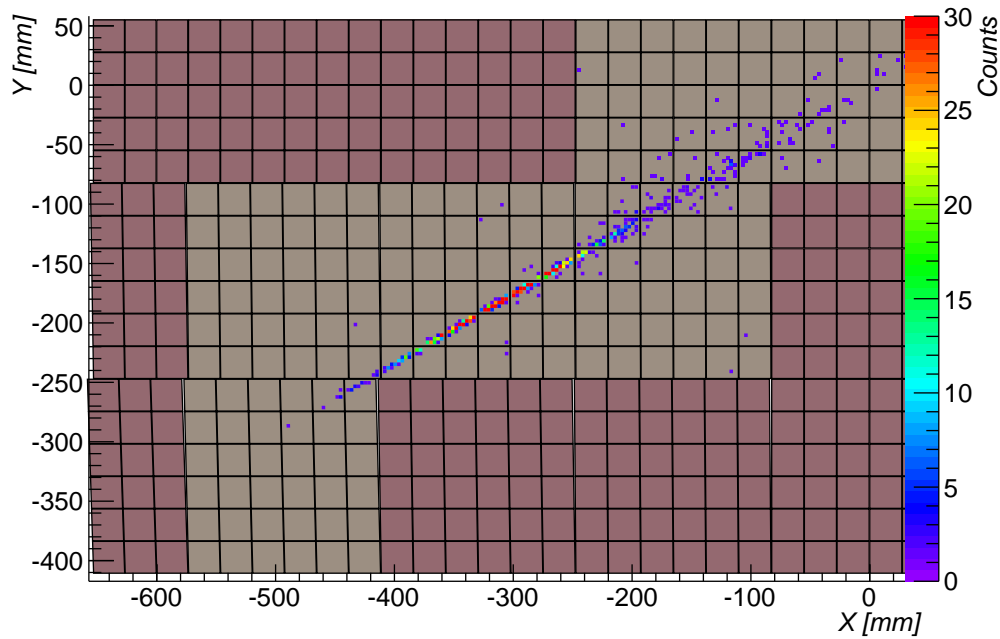
(a) ESAF based shower simulation as similar to figure 6.1a but with enabled Cherenkov lateral distribution taken from [BCC⁺87]. The result shows good agreement with the $\overline{\text{Off}\underline{\text{line}}}$ simulation in figure 6.1b.
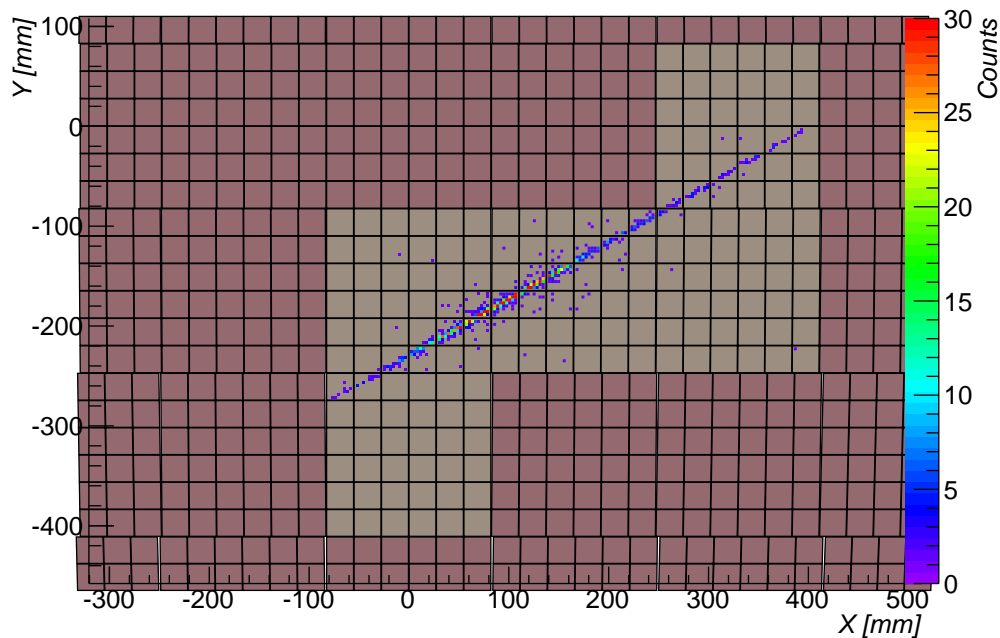
(b) $\overline{\text{Off}\underline{\text{line}}}$ simulation similar to figure 6.1b but with disabled Cherenkov lateral distribution. The result is quite similar with the ESAF simulation 6.1a but $\overline{\text{Off}\underline{\text{line}}}$ also displays a slightly wider lateral distribution of florescence light.

Figure A.3.: Comparison of non-standard simulation configurations of an inclined air shower ($E = 10^{20}$ eV, $\theta = 84°$, $\phi = 30°$, proton) with the same parameters as in figure 6.1.

Bibliography

[AAB⁺05] T. Antoni, W. D. Apel, A. F. Badea, K. Bekk, A. Bercuci, J. Blümer, H. Boz-dog, I. M. Brancus, A. Chilingarian, K. Daumiller, P. Doll, R. Engel, J. Engler, F. Feßler, H. J. Gils, R. Glasstetter, A. Haungs, D. Heck, J. R. Hörandel, K.-H. Kampert, H. O. Klages, G. Maier, H. J. Mathes, H. J. Mayer, J. Milke, M. Müller, R. Obenland, J. Oehlschläger, S. Ostapchenko, M. Petcu, H. Rebel, A. Risse, M. Risse, M. Roth, G. Schatz, H. Schieler, J. Scholz, T. Thouw, H. Ulrich, J. van Buren, A. Vardanyan, A. Weindl, J. Wochele, and J. Zabierowski. KASCADE measurements of energy spectra for elemental groups of cosmic rays: Results and open problems. *Astroparticle Physics*, 24:1–25, September 2005.

[AAVB⁺11] The KASCADE-Grande Collaboration: W. D. Apel, J. C. Arteaga-Velazquez, K. Bekk, M. Bertaina, J. Bluemer, H. Bozdog, I. M. Brancus, P. Buchholz, E. Can-toni3, A. Chiavassa, F. Cossavella, K. Daumiller, V. de Souza, F. Di Pierro, P. Doll, R. Engel, J. Engler, M. Finger, D. Fuhrmann, P. L. Ghia, H. J. Gils, R. Glasstetter, C. Grupen, A. Haungs, D. Heck, J. R. Hoerandel, D. Huber, T. Huege, P. G. Isar, K. H. Kampert, D. Kang, H. O. Klages, K. Link, P. Luczak, M. Ludwig, H. J. Mathes, H. J. Mayer, M. Melissas, J. Milke, B. Mitrica, C. Morello, G. Navarra, J. Oehlschlaeger, S. Ostapchenko, S. Over, N. Palmieri, M. Petcu, T. Pierog, H. Rebel, M. Roth, H. Schieler, F. G. Schroeder, O. Sima, G. Toma, G. C. Trinchero, H. Ulrich, A. Weindl, J. Wochele, M. Wommer, and J. Zabierowski. Kneelike structure in the spectrum of the heavy component of cosmic rays observed with kascade-grande. July 2011.

[ABG⁺07] S. Argiro, S. L. C. Barroso, J. Gonzalez, L. Nellen, T. Paul, T. A. Porter, L. Prado Jr., M. Roth, R. Ulrich, and D. Veberič. The offline software framework of the pierre auger observatory. *Nucl. Instrum. Meth.*, A580:1485–1496, 2007.

[Abr08] Abraham, J, *et al.* (Pierre Auger Collab.). Observation of the suppression of the flux of cosmic rays above 4×10^{19} eV. *Phys. Rev. Lett.*, 101:061101, 2008. arXiv astro-ph/0806.4302.

[ADE⁺12] P. Assis, D. D'Urso, R. Engel, P. Gonçalves, F. Guarino, S. Müller, L. Nozka, S. Petrera, M. Pimenta, F. Salamida, F. Schüssler, B. Tomé, R. Ulrich, M. Unger, and L. Valore. FD simulation, offline reference manual. Auger internal note, 2012.

[AEM⁺39] Pierre Auger, P. Ehrenfest, R. Maze, J. Daudin, and Robley A. Fréon. Extensive cosmic-ray showers. *Rev. Mod. Phys.*, 11(3-4):288–291, Jul 1939.

[BB07] D. Bergman and J. Belz. Cosmic Rays: The Second Knee and Beyond. *J.Phys.G*, 34:R359,2007, April 2007.

Bibliography

[BBM⁺09]   C. Berat, S. Bottai, D. De Marco, S. Moreggia, D. Naumov, M. Pallavicini, R. Pesce, A. Petrolini, A. Stutz, E. Taddei, and A. Thea. ESAF: Full simulation of space-based extensive air showers detectors. *Astroparticle Physics Volume*, 33:221–247, July 2009.

[BCC⁺87]   R. M. Baltrusaitis, G. L. Cassiday, R. Cooper, B. R. Dawson, J. W. Elbert, B. Fick, P. R. Gerhardy, S. Ko, D. F. Liebing, E. C. Loh, Y. Mizumoto, D. Steck, P. Sokolsky, and M. Ye. Measurement of the angular distribution of Cerenkov light in ultra-high-energy extensive air showers. *Journal of Physics G Nuclear Physics*, 13:115–119, January 1987.

[BEH⁺07]   T. Bergmann, Ralph Engel, Dieter Heck, N. N. Kalmykov, S. S. Ostapchenko, Tanguy Pierog, T. Thouw, Klaus Werner, T. Bergmann, R. Engel, D. Heck, N.N. Kalmykov, S. Ostapchenko, T. Pierog, T. Thouw, and K. Werner. One-dimensional Hybrid Approach to Extensive Air Shower Simulation. *Astropart. Phys.*, 26(6):420 – 432, 2007. astro-ph/0606564.

[BEH09]   J. Blümer, R. Engel, and J. R. Hörandel. Cosmic Rays from the Knee to the Highest Energies. arXiv astro-ph/0904.0725, 2009.

[Ber09]   Berg, A. M. van den *et al.* (Pierre Auger Collab.). Radio detection of cosmic rays at the southern Auger Observatory. In *Proc. 31st Int. Cosmic Ray Conf.*, 2009.

[CRE02]   J. Candia, E. Roulet, and L. N. Epele. Turbulent diffusion and drift in galactic magnetic fields and the explanation of the knee in the cosmic ray spectrum. *Journal of High Energy Physics*, 12:33, December 2002.

[EUS04]   EUSO Collaboration. EUSO Red Book, Report on the Phase A Study, 2004. EUSO-PI-REP-005.

[Fo05]   H. Falcke and (LOPES Collaboration) others. Detection and imaging of atmospheric radio flashes from cosmic ray air showers. *Nature*, 435(7040):313–316, 2005.

[GEH⁺06]   D. Góra, R. Engel, D. Heck, P. Homola, H. Klages, J. Pȩkala, M. Risse, B. Wilczyńska, and H. Wilczyński. Universal lateral distribution of energy deposit in air showers and its application to shower reconstruction. *Astroparticle Physics*, 24:484–494, January 2006.

[Gre66]   Kenneth Greisen. End to the cosmic-ray spectrum? *Phys. Rev. Lett.*, 16(17):748–750, Apr 1966.

[Gru10]   Claus Grupen. *Astroparticle Physics*. Springer, 2010.

[Hes12]   V. F. Hess. Beobachtungen der durchdringenden Strahlung bei sieben Freiballonfahrten. *Phys. Z.*, 13:1084, 1912.

[HKC⁺98]   D. Heck, J. Knapp, J.N. Capdevielle, G. Schatz, and T. Thouw. Corsika: A monte carlo code to simulate extensive air showers. Report FZKA 6019, Karlsruhe, 1998.

[HRR03]   A. Haungs, H. Rebel, and M. Roth. Energy spectrum and mass composition of high-energy cosmic rays. *Reports on Progress in Physics*, 66:1145–1206, July 2003.

[JEM10]   JEM-EUSO Collaboration. Report on the Phase A study, 2010.

[KAB⁺04]   B. A. Khrenov, V. V. Alexandrov, D. I. Bugrov, G. K. Garipov, N. N. Kalmykov, M. I. Panasyuk, S. A. Sharakin, A. A. Silaev, I. V. Yashin, V. M. Grebenyuk, D. V. Naumov, A. G. Olshevsky, B. M. Sabirov, R. N. Semenov, M. Slunechka, I. I. Skryl, L. G. Tkatchev, O. A. Saprykin, V. S. Syromyatnikov, V. E. Bitkin, S. A. Eremin, A. I. Matyushkin, F. F. Urmantsev, V. Abrashin, V. Koval, Y. Arakcheev, A. Cordero, O. Martinez, E. Morena, C. Robledo, H. Salazar, L. Villasenor, A. Zepeda, I. Park, M. Shonsky, and J. Zicha. KLYPVE/TUS space experiments for study of ultrahigh-energy cosmic rays. *Physics of Atomic Nuclei*, 67:2058–2061, November 2004.

[Kro94]   P. P. Kronberg. Extragalactic magnetic fields. *Reports on Progress in Physics*, 57:325–382, April 1994.

[Lin79]   J. Linsley. Call for projects and ideas in high energy astrophysics, 1979.

[NKSA03]   M. Nagano, K. Kobayakawa, N. Sakaki, and K. Ando. Photon yields from nitrogen gas and dry air excited by electrons. *Astropart.Phys.*, 20:293–309, 2003.

[OWL]   Orbiting wide-angle light-collectors.

[The06]   A. Thea. *Osservazione di radiazione cosmica di altissima energia dallo spazio*. PhD thesis, Universita degli Studi Di Genova, 2006.

[ZK66]   G. T. Zatsepin and V. A. Kuz'min. Upper Limit of the Spectrum of Cosmic Rays. *JETP Lett.*, 4:78, 1966.

Acknowledgment

I would like to thank Prof. Dr. Johannes Blümer for the opportunity to write my bachelor thesis at the IEKP and for acting as referee.

For his constant support and constructive questions, I would like to thank Dr. Andreas Haungs as active co-referee and advisor. He gave me the opportunity to attend and actively contribute to my first scientific conference.

Deep gratitudes go to whole "FD corridor" and especially Ralf Ulrich for giving me a warm welcome in $\overline{\text{Off}}\underline{\text{line}}$ and answering all my questions.

Furthermore, I would like to thank Tanguy Pierog for my first introduction to air showers and QCD, for his explanations have provided me with a great start into the world of cosmic rays.

My deepest gratitude goes to Dmitry Naumov at the Joint Institute for Nuclear Research (JINR), Dubna for his great support in understanding ESAF and his friendship whenever we met.

I also like to thank Elisabeth Leowardi for pointing out the subtle quirks of the English language.

Special thanks go to Miriam who has always supported me wherever she could, in Physics, physical and non-physical matters.

Finally, I would like to thank my parents and my brother for their support, contributions and means of distraction.

Eidesstattliche Erklärung

Ich erkläre hiermit, dass ich die vorliegende Bachelorarbeit selbständig und ohne uner-
laubte Hilfsmittel angefertigt, andere als die angegebenen Quellen und Hilfsmittel nicht
benutzt und die den benutzten Quellen wörtlich oder inhaltlich entnommenen Stellen als
solche kenntlich gemacht habe. Die Arbeit wurde bisher in gleicher oder ähnlicher Form
oder auszugsweise noch keiner anderen Prüfungsbehörde vorgelegt und auch nicht veröf-
fentlicht.

Karlsruhe, den 23.03.2012

_____

Matthias Blaicher